

## THE STEADY STATE ICE LAYER PROFILE ON A CONSTANT TEMPERATURE PLATE IN A FORCED CONVECTION FLOW—I. LAMINAR REGIME

T. HIRATA, R. R. GILPIN, K. C. CHENG and E. M. GATES

Department of Mechanical Engineering, University of Alberta, Edmonton, Alberta, Canada T6G 2G8

(Received 13 October 1978 and in revised form 23 March 1979)

**Abstract**—The shape of the steady state ice layer that forms on a constant temperature horizontal plate in a parallel forced convection flow was analyzed. This paper, part I of a two part series, will examine phenomena that effect the shape of the ice layer in the laminar flow regime. Of particular interest are the effects of curvature of the ice surface on the free stream flow and of streamwise heat conduction in the ice layer. A two-dimensional theory developed to account for these effects suggests that a modified Reynolds number of the form  $Re_w/\theta_c^2$  where  $\theta_c$  is a temperature ratio parameter should be used to correlate the ice profiles. It was found that measurements could be correlated over a wide range of plate temperatures, free stream temperatures and free stream velocities using this parameter. Also in the laminar regime thermal instabilities of the boundary layer were observed which produced longitudinal grooves in the ice surface.

### NOMENCLATURE

$C, C_1, C_2, C_3$ , constants defined in equations (5) and (14);  
 $C_p$ , specific heat;  
 $Gr$ , Grashof number based on characteristic thickness of boundary layer, equation (25);  
 $Nu_x$ , local Nusselt number,  $hx/\lambda_w$ ;  
 $Pr$ , Prandtl number;  
 $Re_x$ , Reynolds number,  $U_\infty x/\nu$ ;  
 $St$ , Stanton number, equation (14);  
 $T_f, T_w, T_\infty$ , freezing, plate and free stream temperatures;  
 $U_{\infty 0}, U_\infty$ , free stream velocity far from ice surface; velocity parallel to ice surface outside viscous boundary layer;  
 $V$ , complex velocity;  
 $a$ , distance between leading edge of ice surface and leading edge of plate;  
 $g$ , acceleration due to gravity;  
 $h(s)$ , local heat transfer coefficient;  
 $q, q_i, q_w, q_s$ , heat flux, heat flux in ice, heat flux in water, heat flux normal to ice surface;  
 $s$ , distance from leading edge of ice measured along ice surface;  
 $x'$ , distance from leading edge of ice measured parallel to plate,  $x + a$ ;  
 $y'$ , distance normal to plate measured from ice surface;  
 $x, y$ , distance parallel to plate measured from its leading edge and distance normal to plate from its surface;  
 $w, z, \zeta$ , complex coordinates,  $\phi + i\psi$ ,  $x + iy$  and  $\xi + i\eta$ ;  
 $\delta_i$ , ice thickness;  
 $\eta, \xi$ , parabolic coordinates;  
 $\theta, \theta_c$ , non-dimensional temperature  $(T - T_w)/(T_f - T_w)$ , cooling temperature ratio,  $(T_f - T_w)/(T_\infty - T_f)$ ;

$\lambda_i, \lambda_w$ , ice and water thermal conductivities;  
 $\nu$ , kinematic viscosity;  
 $\rho$ , density;  
 $1 - D, 2 - D$ , values for one-dimensional and two-dimensional theories.

### INTRODUCTION

PROBLEMS involving the growth or decay of the solid phase of a substance have generally come to be called "Stefan-like" problems. These problems occur in a wide range of practical applications including the formation of an ice cover, the casting of a metal, the ablation of a heat shield, and the deposition of a frost layer on a cold surface to name only a few. One common characteristic of the Stefan-like problems is that phase change and an associated source or sink of latent heat occurs at the moving interface. This produces a non-linear character in the transient part of these problems which causes much of the computational difficulty associated with them. In the original study of the formation of an ice cover done by Stefan only conduction heat transfer was involved [1]. Since then the effects of radiation [2], free convection [3, 4] and forced convection [5–14] have been studied. In problems where a convective flow occurs at the phase change interface, besides the basic non-linearity of the transient problem, two additional complications arise. First, since the specific volumes of the solid and the fluid phases are seldom the same, the phase change at the interface is equivalent to an effective suction or blowing at the surface. This effect, which of course alters the heat transfer coefficient at the phase change surface, has been examined in a number of different situations [4, 9–14]. The second complication arises because, in these convective problems, a mutual interaction occurs among the shape of the phase change

interface, the flow field next to it, and the heat transfer from the flow to the interface. Theoretical studies of the interaction of the flow field and the ice interface shape have so far been restricted to several laminar flow problems with relatively simple geometry. These problems include the solidification in a parallel plate channel [15, 16] and in a pipe [17], the penetration of ice by a water jet [14], and various problems which combine free convection and solidification [3, 18, 19].

For a constant temperature plate in a semi-infinite forced convection flow analytical studies have primarily concentrated on examining the non-linear nature of the transient ice formation problem [5-7]. In these calculations the ice layers formed are assumed to be thin enough so that stream-wise heat conduction in the ice and effects of the ice layer on the flow over the plate can be neglected. Several approaches have been tried to approximate the effects that a thick ice layer would have [18, 19]. The result of these analyses will be discussed later in the paper.

In this paper the phenomena that determine the steady state shape of the ice layer of a flat, constant temperature plate in a forced convection flow will be examined. Since the results will only be concerned with the final steady state ice layer the transient aspects of the Stefan's problem will not enter the discussions. The phase change characteristic which will be of most interest in this study is the interaction of the flow field and the ice layer shape. To emphasize this effect the measured ice shapes will be compared with those predicted by a simple one-dimensional analysis which assumes the ice layer is very thin and has no effect on the flow field or heat transfer rate. The ice layer profile that exists in the laminar regime will be examined in this paper, Part I. The following paper, Part II, will deal with the transition to turbulence and the turbulent regime.

#### EXPERIMENTAL APPARATUS AND PROCEDURE

The present experimental work was carried out in a closed loop water tunnel having a test section with dimensions 25.4 cm (width)  $\times$  45.7 cm (height)  $\times$  213.4 cm (length). The temperature of the water in the tunnel could be controlled by means of a refrigeration and heat exchanger system at any value between room temperature and 0°C. A copper plate 6.35 mm thick, 24.1 cm wide and 152 cm long was installed horizontally in the test section with its cold surface facing upward. This plate was used for the purpose of ice growth, with its temperature being maintained isothermal and uniform by circulating a coolant fluid from a temperature controlled bath at a high velocity under the plate. Thus, the plate temperature could be controlled at any point between 0 to -19°C, independent of the free stream temperature. Consequently, it was possible to grow ice on the plate under uniform temperature and velocity conditions of the free stream flow, at various sets of experimental conditions. Figures showing the

overall construction of this facility were presented in [22]. Figure 1 of this paper shows a detail of the configuration of main flow, coolant flow and ice formation near the leading edge of the plate. It will be noted that the ice is shown growing in front of the leading edge of the plate. This was predicted by the theory and observed experimentally. In the experimental configuration used the suction under the plate could be adjusted so that the flow approaching the leading edge of the plate was parallel to it. Also as an ice build-up occurred on the plate the suction could be adjusted to maintain the stagnation point of the flow at the leading edge of the ice profile.

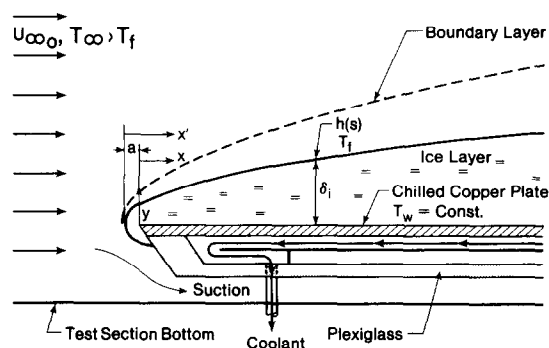


FIG. 1. Schematic representation of the ice layer profile, the coolant flow and the main flow in the vicinity of the leading edge of the cooling plate.

In order to measure velocity profiles above the ice, a laser Doppler anemometer with a helium-neon gas laser (15 mW output) in the forward scatter mode was used. Frequency shifting was employed on one of the beams to improve the doppler signals. The laser optics were mounted on a three-dimensional traversing rig driven by stepping motors and controlled by a programable calculator. With this system velocity profiles could be measured at various distances from the leading edge of the plate. The laser traversing rig was also used to measure the position of the ice surface. This was done by moving the traversing head so that the laser beam coincided with the ice-water interface at various positions along the ice profile. The coordinates of these points when compared to coordinates of a reference line on the test section window could then be used to give the ice thickness profile. The laser doppler signal was also analyzed to give an indication of the free stream turbulence level.

Vertical temperature profiles in the boundary layer were taken using a 51  $\mu$ m dia copper-constantan thermocouple formed in the shape of a loop which could also be traversed through the boundary layer. All data were taken after a thermally steady state was confirmed.

The ranges of conditions employed were:

- free stream velocity  $U_\infty = 4.3 \sim 15$  cm/s
- free stream temperature  $T_\infty = 1.3 \sim 5.0^\circ\text{C}$
- plate temperature  $T_w = -2.3 \sim -12.4^\circ\text{C}$ .

Consequently the range of parameters covered by these test conditions were  $Re_x = 2 \times 10^2 \sim 10^5$  and the cooling temperature ratio  $\theta_c = 1.6 \sim 9.5$ .

**THEORETICAL PREDICTION OF THE STEADY STATE ICE LAYER ON A CONSTANT TEMPERATURE PLATE**

The problem to be considered is that of freezing of water on a cold surface in a steady plane flow as shown in Fig. 1. The local thickness of the ice layer is  $\delta_i$  and its thermal conductivity is  $\lambda_i$ . The temperature of the cold surface is  $T_w$ , which is below the freezing temperature,  $T_f$ .

(a) *Simple one-dimensional theory*

First a simple one-dimensional analysis will be presented in which the thickness of the ice layer is assumed to be small. In this limit there is a negligible difference between  $x$  and  $x'$ , that is  $a = 0$ , and the temperature profile through the ice can be assumed to be linear. The conductive heat flux,  $q_i$ , through the ice is then

$$q_i = \lambda_i \frac{T_f - T_w}{\delta_i}.$$

Also if  $\delta_i$  is small the heat-transfer coefficient,  $h(s)$ , to the ice surface can be assumed to be unaffected by the shape of the ice surface. The convective heat flux,  $q_w$ , transferred from the water to the ice interface is then given by

$$q_w = h(T_\infty - T_f)$$

where  $h$  is the heat-transfer coefficient on a flat plate with no ice layer and  $T_\infty$  is the free stream temperature. The heat balance equation at the ice interface is:

$$h(T_\infty - T_f) = \lambda_i \frac{T_f - T_w}{\delta_i} \quad (1)$$

or in terms of a local Nusselt number equation (1) can be written

$$\frac{x}{\delta_i} = \frac{\lambda_w}{\lambda_i} \frac{T_\infty - T_f}{T_f - T_w} Nu_x. \quad (2)$$

Equation (2) could be used to predict the ice thickness if the Nusselt number is known or alternatively the local Nusselt number could be calculated using measured values of the ice thickness.

For a laminar boundary-layer flow on a flat plate, the local Nusselt number is given by [23]

$$Nu_x = 0.332 Pr^{1/3} Re_x^{1/2}. \quad (3)$$

Using this expression in equation (2) gives

$$\frac{x}{\delta_i} = \frac{\lambda_w}{\lambda_i} 0.332 Pr^{1/3} Re_x^{1/2} / \theta_c \quad (4)$$

where  $\theta_c$  is the cooling temperature ratio,  $(T_f - T_w)/(T_\infty - T_f)$ . The reciprocal of this ratio,  $1/\theta_c$ , is sometimes referred to as the superheat ratio. The prediction in equation (4) is applicable only if the ice layer has grown to its steady state profile, the flow is laminar and unaffected by the shape of the ice layer

and if streamwise heat conduction in the ice layer is negligible. The result in equation (4) will be compared to the result of a two-dimensional analysis to follow where some of the above restrictions have been relaxed.

(b) *Two-dimensional theory*

The effects of two of the approximations used in deriving equation (4), the effects of the shape of the ice layer on free stream flow and the effect of streamwise heat conduction in the ice, will now be analyzed using a two-dimensional model of the ice layer and the flow around it. Rearranging equation (4) gives

$$\delta_i^2 = Cx \quad (5)$$

where

$$C = \left( \frac{\lambda_i}{\lambda_w} \frac{\theta_c}{0.332 Pr^{1/3}} \right)^2 \frac{v}{U_\infty}.$$

That is the shape of the ice surface is, at least for small ice thicknesses, a parabola. This observation suggests a basis for an analytic solution of the two dimensional problem. It will be assumed that in the case of large ice thicknesses the shape of the ice layer is still approximately parabolic. The solutions for the heat conduction in the ice and the free stream flow can then be readily obtained using a transformation to parabolic coordinates. The definition of symbols for the two-dimensional problem are shown in Fig. 2.

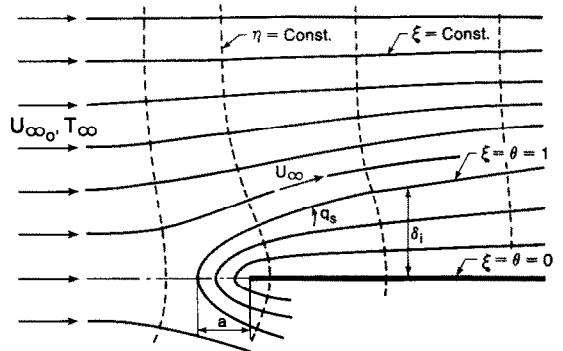


FIG. 2. Coordinate system for solving the heat-conduction equation in the ice and the potential flow equation exterior to the ice.

It will be noted that for this problem the ice surface is assumed to be a parabola with its vertex displaced a distance  $a$ , in front of the leading edge of the plate. This distance  $a$ , will be calculated and used in the solution.

First the heat-conduction problem in the ice will be solved. Applying the complex transformation

$$z = -a\zeta^2 \quad (6)$$

where

$$z = x + iy \text{ and } \zeta = \xi + i\eta$$

transforms the parabolic ice layer into a plane slab. The original and transformed coordinates are related by

$$x = -a(\xi^2 - \eta^2) \quad (7)$$

$$\text{and } y = -2a\xi\eta.$$

On the cooling plate,  $\xi = 0, \theta = 0$  where  $\theta = (T - T_w) / (T_f - T_w)$ . On the ice-water interface,  $\xi = 1, \theta = 1$ . Also on  $\xi = 1$  which defines  $\delta_i = y$ , equation (7) gives  $\delta_i^2 = 4a(a+x)$ .

It will generally be more convenient to use an  $x'$  coordinate  $x' = a+x$ , defined from the leading edge of the ice so that

$$\delta_i^2 = 4ax'. \tag{8}$$

In the transformed coordinates the solution for the temperature field,  $\nabla^2\theta = 0$ , is just

$$\theta = \xi. \tag{9}$$

Transformed back to  $x, y$  coordinates this gives

$$\theta = \left( \frac{-x + (x^2 + y^2)^{1/2}}{2a} \right)^{1/2} \tag{10}$$

For this problem the heat flux at the ice-water interface is of more interest than the temperature field itself.

The complex heat flux is

$$q = q_x + iq_y = -\lambda_i(T_f - T_w) \frac{d\theta}{dz}.$$

Its magnitude,  $|q| = (q\bar{q})^{1/2}$ , at the surface  $\xi = 1$  is

$$q_s = \lambda_i(T_f - T_w) \frac{1}{2a(1+\eta^2)^{1/2}}.$$

Using equation (7) and (8) to express this in terms of  $\delta_i$  and  $x'$  gives the desired result

$$q_s = -\lambda_i \frac{(T_f - T_w)}{\delta_i} \frac{1}{(1 + (\delta_i/2x')^2)^{1/2}}. \tag{11}$$

As would be expected when  $\delta_i/x' \ll 1$  equation (11) approaches the one-dimensional result.

To solve for the heat-transfer coefficient exterior to the ice layer the potential flow over the ice surface

must first be obtained. In the transformed coordinates used above the flow of a uniform stream over the parabolic ice surface becomes a stagnation flow impinging normally on a flat surface. The complex potential for such a flow is given by

$$w(\zeta) = \phi + i\psi = U_{\infty 0} a (\zeta^2 - 2\zeta) = U_{\infty 0} a \{ [\zeta^2 - \eta^2 - 2\zeta] + i2(\zeta - 1)\eta \} \tag{12}$$

where  $U_{\infty 0}$  is the uniform stream velocity far from the ice surface [24]. From equation (12) it can be seen that  $\xi = 1$  is a streamline with  $\psi = 0$ . The required result is the magnitude of the velocity  $U_{\infty}$ , along this streamline. The complex velocity,  $V = dw/dz$ , is

$$V = U_{\infty 0} \left( \frac{1 - \zeta}{\zeta} \right).$$

The magnitude of the velocity,  $|V| = (V\bar{V})^{1/2}$ , on  $\xi = 1$  is then

$$U_{\infty} = U_{\infty 0} \frac{\eta}{(1 + \eta^2)^{1/2}}. \tag{13}$$

For a boundary layer growing with varying free stream velocity an approximate means of calculating the heat-transfer coefficient has been developed using the wedge solutions. This procedure is described in, for example, Kays [25]. The result is that the Stanton number,  $St$ , is given by

$$St_s = \frac{C_1 v^{1/2} (U_{\infty})^{C_2}}{\left( \int_0^s (U_{\infty})^{C_3} ds \right)^{1/2}}. \tag{14}$$

For  $Pr = 10$  values of the constants are given as  $C_1 = 0.073, C_2 = 0.685,$  and  $C_3 = 2.37$ . The velocity in equation (13) can be substituted into equation (14) and the integration carried out to give the heat-transfer coefficient as a function of position along the ice surface. In carrying out the integration it will be more convenient to convert the integral into an integral over  $\eta$  rather than  $s$ . For this purpose  $ds/d\eta = 2a(1 + \eta^2)^{1/2}$  may be used. The result is that

$$h(s) = \frac{0.073 v^{1/2} \rho C_p U_{\infty 0}^{1/2}}{(2a)^{1/2} (1 + \eta^2)^{0.8425}} \frac{\eta^{1.685}}{\left[ \int_0^{\eta} \frac{\eta'^{2.37} d\eta'}{(1 + \eta'^2)^{0.685}} \right]^{0.5}}. \tag{15}$$

The heat-transfer coefficient can be expressed as a function of  $\delta_i$  and  $x'$  noting that  $a = \delta_i^2/(4x')$  and  $\eta = 2x'/\delta_i$ .

A heat balance at the ice surface can now be used to relate  $q_s$  and  $h(s)$

$$-q_s ds = h(s)(T_{\infty} - T_f) ds. \tag{16}$$

Inserting equation (11) and (15) in equation (16) and rearranging the result gives

$$\frac{x'}{\delta_i} = \frac{\lambda_w}{\lambda_i} \frac{0.730}{\theta_c} \left( \frac{U_{\infty 0} x'}{v} \right)^{0.5} \left( 1 + f \left( \frac{x'}{\delta_i} \right) \right) \tag{17}$$

where

$$f \left( \frac{x'}{\delta_i} \right) = \frac{\left( \frac{2x'}{\delta_i} \right)^{1.685}}{\sqrt{2} \left[ 1 + \left( \frac{2x'}{\delta_i} \right)^2 \right]^{0.3425}} \left[ \int_0^{2x'/\delta_i} \frac{\eta'^{2.37}}{(1 + \eta'^2)^{0.685}} d\eta' \right]^{0.5} - 1 \tag{18}$$

Near the leading edge of the plate where  $x'/\delta_i \ll 1$

$$f\left(\frac{x'}{\delta_i}\right) \approx \left(\frac{3.37}{2}\right)^{1/2} - 1 = 0.2981. \quad (19)$$

Equation (17) then predicts that the ice has a parabolic shape given by

$$\frac{x'}{\delta_i} = 0.948 \frac{\lambda_w}{\lambda_i} Re_x^{0.5} / \theta_c. \quad (20)$$

From this expression the distance  $a$ , that the ice forms in front of the plate can be obtained

$$a = \frac{\delta_i^2}{4x'} = 0.278 \left(\frac{\lambda_i}{\lambda_w} \theta_c\right)^2 \frac{v}{U_{\infty 0}}. \quad (21)$$

Alternatively for  $x \approx x'$ ,  $f(x'/\delta_i) = 0$  and equation (17) gives

$$\frac{x}{\delta_i} = 0.730 \frac{\lambda_w}{\lambda_i} Re_x^{0.5} / \theta_c. \quad (22)$$

Except for a slight difference in the constant 0.730 this is the same as the one-dimensional result in equation (4). Referring back to equation (13) it can be seen that for large distances,  $\eta$ , from the stagnation point the stagnation flows gives a constant free stream velocity  $U_{\infty 0}$  which is the same condition as that for parallel flow over a flat plate.

If the result of equation (22) is defined as  $(x/\delta_i)|_{1-D}$  equation (17) can be rewritten as

$$\frac{x}{\delta_i}|_{2-D} = \frac{x}{\delta_i}|_{1-D} \left(\frac{x}{x'}\right)^{0.5} \left[1 + f\left(\frac{x'}{\delta_i}\right)\right] \quad (23)$$

where  $(x/\delta_i)|_{2-D}$  is the result including the two-dimensional effect. The function  $f(x'/\delta_i)$  was obtained by numerically integrating equation (18). The result is shown in Fig. 3. Since  $f(x'/\delta_i)$  is only a small correction factor in equation (23) it was found that its effect could satisfactorily be approximated by substituting  $(x/\delta_i)|_{1-D}$  for  $x'/\delta_i$  in the function. The difference between  $x$  and  $x'$  will still enter into the first order term  $(x/x')^{0.5}$ . Here the ratio  $x/x'$  can also

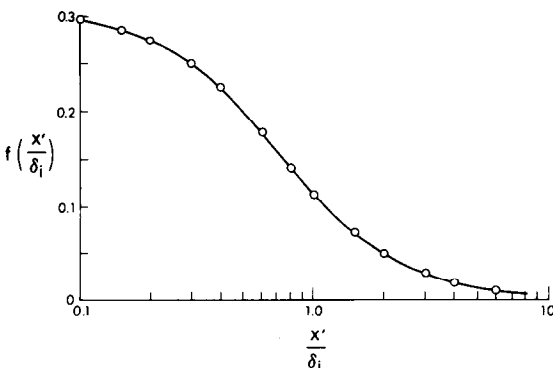


FIG. 3. The function,  $f(x'/\delta_i)$ , in the two dimensional theory solved for by numerical integration.

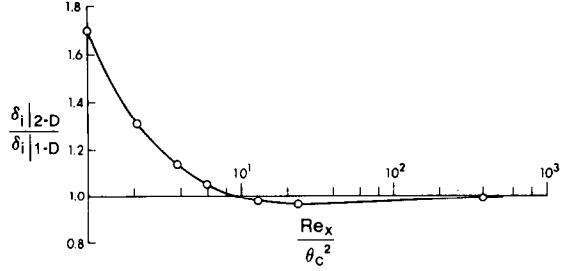


FIG. 4. A comparison of the ice thicknesses predicted by the two-dimensional and one-dimensional theories.

be related to  $(x/\delta_i)|_{1-D}$  by using equation (21). With these substitutions equation (23) becomes

$$\frac{x}{\delta_i}|_{2-D} = \frac{x}{\delta_i}|_{1-D} \frac{\left[1 + f\left(\frac{x}{\delta_i}|_{1-D}\right)\right]}{\left[1 + 0.148 \left(\frac{\delta_i}{x}|_{1-D}\right)^2\right]^{0.5}}. \quad (24)$$

The result  $(x/\delta_i)|_{2-D}$  is then given as an explicit function of  $(x/\delta_i)|_{1-D}$  or alternatively using equation (4) or (22) it can be seen that  $(x/\delta_i)|_{2-D}$  is an explicit function of  $Re_x/\theta_c^2$ . The ratio  $\delta_i|_{2-D}/\delta_i|_{1-D}$  derived from equation (24) is plotted as a function of  $Re_x/\theta_c^2$  in Fig. 4. For values of  $Re_x/\theta_c^2$  less than about nine the two-dimensional theory predicts a larger ice thickness than the one-dimensional result. This occurs because the two-dimensional theory accounts for the fact that the ice grows in front of the leading edge of the plate so that the ice thickness does not go to zero at  $x = 0$  as the one-dimensional theory would predict. For  $Re_x/\theta_c^2$  greater than nine the two-dimensional theory predicts an ice layer a few percent thinner than the one-dimensional theory. This thinning of the ice layer is due to the combined effects of streamwise heat conduction in the ice layer and the acceleration of the free stream velocity over the ice surface. These predictions will be compared with experimental results in the next section.

As mentioned in the Introduction several previous attempts have been made to approximate the effects of streamwise heat conduction and free stream acceleration. Saito *et al.* [20] used a heat-transfer correlation for a blunt body of arbitrary shape and a distributed source model for approximating the flow and heat transfer to the ice surface on a plate. In this analysis the possibility that the ice could form in front of the leading edge of the plate was neglected. Introducing this approximation,  $x = x'$ , into equation (20) gives a result within 1% of the result in [20] for the shape of the ice surface near the leading edge of the ice sheet. The heat-transfer correlation used in [20] does not approach the flat plate correlation for large values of  $x$  so that the resulting expression may be expected to apply only near the leading edge.

The results of the other attempt to analyze the effect of a thick ice sheet [21], appeared to have some basic inconsistencies in it; however, that result could not be put in a form which could be checked against the present results.

RESULTS

Measured ice profile thicknesses for several different temperature and velocity conditions are shown in Fig. 5. The ice thicknesses shown, up to 10 cm, were typical of those within the accessible range of experimental parameters. The figure also shows that for the thicker ice layers the ice does in fact extend in front of the leading edge of the plate as was predicted by the two-dimensional theory. In this figure the two independent effects of velocity and temperature are shown. The theory of the previous section suggests,

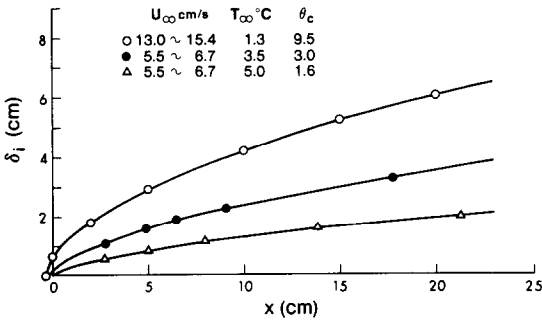


FIG. 5. Measured ice layer profiles for several conditions of free stream velocity and temperature ratio.

however, that these effects can be combined in the single parameter  $Re_x/\theta_c^2$ . This will be done later but first the velocity and temperature profiles over the ice will be examined.

Figures 6 and 7 show respectively the dimensionless velocity and temperature profiles above the ice surface for various values of  $Re_x/\theta_c^2$ . It should also be noted that for both of these profiles the scanning apparatus was restricted to operation in the vertical plane and thus the distance  $y'$ , in the figures is a vertical distance from the ice surface and not a distance normal to the ice as might have been preferred. In the figures this distance has been normalized by the characteristic laminar boundary-layer thickness,  $(\nu x/U_{\infty 0})^{0.5}$ , so that for a boundary layer developing on a flat plate all the profiles should fall on a single curve marked "laminar theory for flat plate". Comparison of the measured profiles with the flat plate profiles; therefore, shows the effects of the ice surface.

In Fig. 6 it should be noted that the viscous boundary layer is confined to values of the dimensionless  $y$  distances of about 5 or less. Outside this

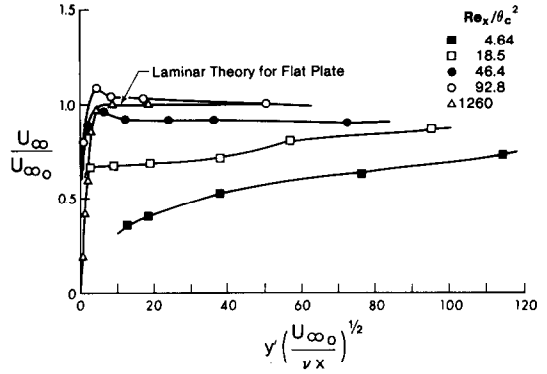


FIG. 6. Measured velocity profiles near the ice surface with  $U_{x,0} = 12.6$  cm/s,  $T_{\infty} = 1.32$  °C and  $\theta_c = 8.86$ .

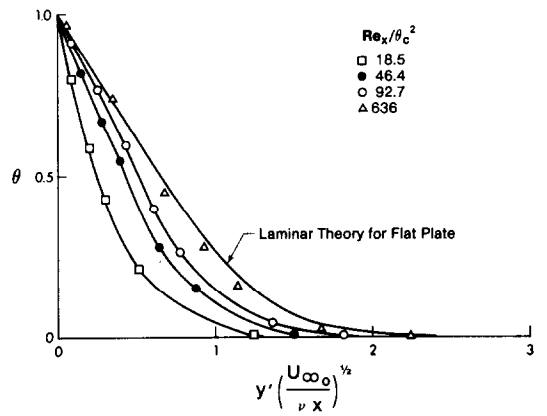


FIG. 7. Measured temperature profiles near the ice surface with  $U_{x,0} = 12.6$  cm/s,  $T_{\infty} = 1.32$  °C and  $\theta_c = 8.86$ .

This again is a result of the flow acceleration. The profile at  $Re_x/\theta_c^2 = 92.8$  suggests that the velocity at this maximum is actually slightly larger than the free stream value far from the ice. This may in fact be an experimental artifact. For very large values of  $Re_x/\theta_c^2$  the profile does, however, approach that for a flat plate.

The anticipated effect of the free stream acceleration on the temperature profile is to increase the temperature gradient at the ice surface. Such an increase is observed in Fig. 7; however, it must be remembered that to obtain the actual temperature gradient normal to the ice surface a correction must first be made for the local slope of the ice profile.

In Fig. 8 the measured ice profiles are compared with the one- and two-dimensional theories of the previous section. In this figure the results have been

appropriate to use in the boundary-layer calculation is the value just outside the rapid drop in velocity at the ice surface. The profiles taken near the leading edge,  $Re_x/\theta_c^2 = 4.64$  and  $18.5$  show that this value of  $U_{\infty}$  is increasing rapidly with  $Re_x/\theta_c^2$  as the velocity accelerates from the stagnation point on the ice. For  $Re_x/\theta_c^2 = 46.4$  and  $92.8$  the velocity profiles exhibit a maximum just outside the viscous boundary layer.

show the same general behavior as the two-dimensional theory predicts. That is, for small  $Re_x/\theta_c^2$  the value of  $x/\delta_i$  is less than the one-dimensional prediction. For intermediate values of  $Re_x/\theta_c^2$  the results are above the one-dimensional prediction and for larger values of  $Re_x/\theta_c^2$  the measurements again approach the one-dimensional values. Throughout most of the experimental range the measured values

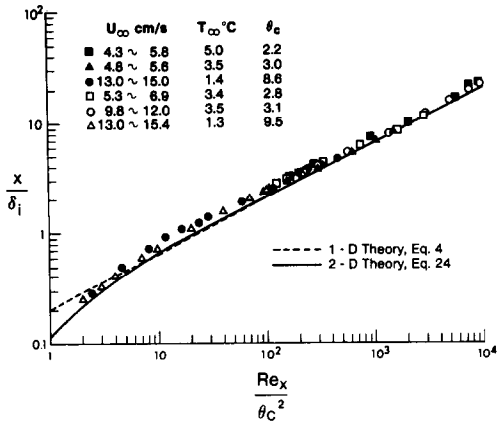


FIG. 8. A comparison of predicted and measured ice layer profiles on a constant temperature plate.

of  $x/\delta_i$  are, however, 10–20% higher, that is, the ice thickness is less than that predicted by the two-dimensional theory.

Several factors could contribute to this discrepancy. As can be seen from Fig. 1 the cooling channels in the constant temperature plate could not be extended right to the leading edge of the plate. Approximately 2 cm of the leading edge is cooled only by conduction in the copper plate. Measurements made by touching a fine thermocouple to the plate surface indicated that the plate was at a constant temperature within the accuracy of the measurement technique for most of its length. However, if the effective leading edge of the constant temperature plate is as much as a few millimeters downstream from the physical edge of the plate the data in Fig. 8 would be shifted downward significantly. Another factor that should be mentioned is that the water tunnel used had a fairly high free stream turbulence level. The RMS fluctuation in  $U_\infty$  was about 1%. This may have contributed to an increased heat-transfer rate to the ice over that which would be predicted for an ideally laminar flow. Kestin [26] has found that free stream turbulence levels have a large effect on laminar heat-transfer rates in regions of accelerating flow but have no effect in regions of zero pressure gradient flow. This would explain the increased heat-transfer rates observed over the initial part of the ice layer in these experiments. The increase in heat-transfer rate observed by Kestin near the stagnation point of a cylinder in cross flow was 30–40% for  $Tu = 0.8\%$ . This magnitude of change in heat-transfer rate is compatible with the measurements on the ice surface.

For the present experimental arrangement of an upward facing ice surface the water between the freezing point,  $0^\circ\text{C}$ , at the ice surface and the maximum density point at  $4^\circ\text{C}$  has an unstable density gradient. That is, the density in the boundary layer is increasing with height above the ice. Previous studies of the laminar boundary-layer flow on a flat plate with no ice have shown that for a sufficiently thick boundary layer the thermal in-

stability generates secondary flows in the boundary layer [22, 27]. These secondary flows take the form of vortices with their axis aligned parallel with the flow direction (longitudinal vortices). The condition for the onset of these vortices in a laminar boundary layer on an ice surface will depend on the free stream temperature,  $T_\infty$ . The most unstable situation exists when  $T_\infty = 4^\circ\text{C}$  in which case the onset of the vortices would occur when a parameter  $Gr \approx 200$  [27]. The parameter  $Gr$  is a Grashof number based on the characteristic thickness of the boundary layer and for  $T_\infty = 4^\circ\text{C}$  it is given by

$$Gr = 2.54 \times 10^{-4} \frac{g}{\nu^2} \frac{x^3}{Re_x^3} \quad (25)$$

For small free stream velocities and large distances along the ice surface the value of  $Gr$  may exceed the critical value for the onset of vortices before the Reynolds number exceeds the critical value for onset of turbulence. For example, with  $U_\infty = 4.0\text{ cm/s}$ ,  $T_\infty = 4^\circ\text{C}$  and at  $x = 100\text{ cm}$  the Reynolds number is  $2.3 \times 10^4$  and  $Gr = 220$ . Under these conditions longitudinal vortices in a laminar boundary layer would be expected. Figure 9 shows the effect of these vortices on the ice surface at the conditions defined above. The effect of the vortices is to produce longitudinal grooves in the ice surface. For the conditions that were obtainable in this experiment the secondary circulation in the vortices is weak and the depth of the grooves in the ice was too small to be measured directly. They were; however, readily discernible by observing the light reflected from the ice surface. Figure 9 shows the reflection of the laser beam light, upper straight line, from the ice surface, lower wavy line. For the length of plate in the present experiment these longitudinal vortices did not develop to a sufficient intensity that they had a measurable effect on the overall ice thickness. It may be, however, that for low velocity flows over a very long ice surface that their effect on the overall heat transfer rate would have to be taken into account.

## CONCLUSIONS

An analysis of the ice growth on a constant temperature plate in forced convection showed that the two-dimensional effects of streamwise heat conduction in the ice and of free stream acceleration over the ice could be modelled by approximating the ice layer as a parabolic cylinder. This analysis showed that the relevant parameter for determining when these effects are important is a modified Reynolds number of the form  $Re_x/\theta_c^2$  where  $\theta_c$  is a temperature ratio parameter. The calculations show that streamwise heat conduction and flow acceleration are significant for  $Re_x/\theta_c^2$  less than about 50. However, due in part to a partial cancellation of the various two-dimensional effects a large difference between the one-dimensional approximation and the two-dimensional analysis occurs only when  $Re_x/\theta_c^2$  is less than about 6. The experimental measurements of the ice thickness generally confirmed this theoretical

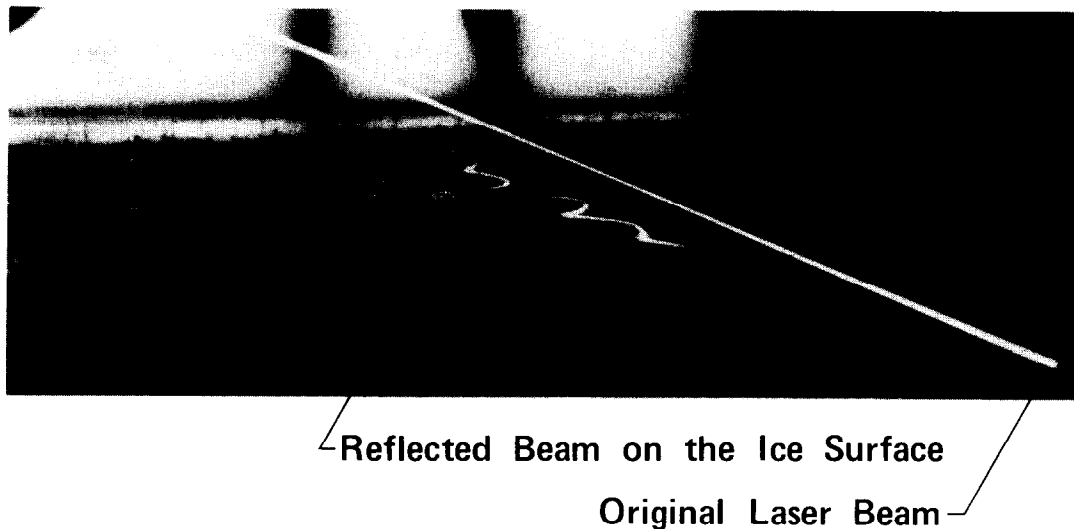


Fig. 9. Photograph showing longitudinal grooves in the ice surface caused by longitudinal vortices with  $U_{\infty 0} = 4.0$  cm/s,  $T_s = 4^\circ\text{C}$  and  $\theta_s = 0.6$  at  $x = 100$  cm.

prediction although there was a 10–20% discrepancy near the plate leading edge. The overall conclusion of the measurements and the calculation is, however, the same. That conclusion is that the one-dimensional approximation will probably be sufficiently accurate for most practical purposes. One significant prediction of the two-dimensional analysis which is not given by the one-dimensional approximation is that the steady state ice layer actually extends upstream of the leading edge of the cooling plate. This prediction was confirmed in the experimental observations.

One other interesting phenomenon that was observed in the experiments was a thermal instability of the boundary layer. For small velocities and at large distances along the plate this thermal instability was observed to produce longitudinal grooves in the ice surface. This phenomenon may be of interest in explaining some surface features of glaciers where surface run-off is present. It should be noted, however, that it will occur only for low velocity flows and only in the case where the flow is over an ice surface.

*Acknowledgement* This work was supported by the National Research Council of Canada. The authors would also like to acknowledge the very capable technical assistance of Mr. D. Beaton in conducting these experiments.

#### REFERENCES

1. J. Stefan, Über die Theorie der Eisbildung, insbesondere über die Eisbildung im Polarmeere, *Ann. Phys. Chem.* **42**, 269–286 (1891).
2. G. S. H. Lock, On the use of asymptotic solutions to plane ice–water problems, *J. Glaciol.* **8**, 285–300 (1969).
3. J. Szekeley and P. S. Chhabra, The effect of natural convection on the shape and movement of the melt–solid interface in controlled solidification of lead, *Metall. Trans.* **1**, 1195–1203 (1970).
4. H. J. Merk, The influence of melting and anomalous expansion on the thermal convection in laminar boundary layers, *Appl. Scient. Res.* **4**, 435–452 (1954).
5. P. A. Libby and S. Chen, The growth of a deposited layer on a cold surface, *Int. J. Heat Mass Transfer* **8**, 395–402 (1965).
6. C. Lapadula and W. K. Mueller, Heat conduction with solidification and a convective boundary condition at the freezing front, *Int. J. Heat Mass Transfer* **9**, 702–704 (1966).
7. K. Stephan, Influence of heat transfer on melting and solidification in forced flow, *Int. J. Heat Mass Transfer* **12**, 199–214 (1969).
8. R. T. Beaubouef and A. J. Chapman, Freezing of fluids in forced flow, *Int. J. Heat Mass Transfer* **10**, 1581–1587 (1967).
9. Y. C. Yen and C. Tien, Laminar heat transfer over a melting plate, the modified Leveque problem, *J. geophys. Res.* **68**, 3673–3678 (1963).
10. R. Siegel and J. M. Savino, An analysis of the transient solidification of a flowing warm liquid on a convectively cooled wall, in *Proc. 3rd Int. Heat Transfer Conf.*, Vol. 4, pp. 141–151. Am. Soc. Mech. Engrs, New York (1966).
11. J. M. Savino and R. Siegel, An analytical solution for solidification of a moving warm liquid onto an isothermal cold wall, *Int. J. Heat Mass Transfer* **12**, 803–809 (1969).
12. J. M. Savino, J. F. Zumdieck and R. Siegel, Experimental study of freezing and melting of flowing warm water at a stagnation point on a cold plate, in *Heat Transfer 1970*, Vol. 1, Cu 2.10. Elsevier, Amsterdam (1970).
13. F. M. Pozvonkov, E. F. Shurgalskii and L. S. Akselrod, Heat transfer at a melting flat surface under conditions
14. R. R. Gilpin and A. W. Lipsett, Impingement melting: experiment and numerical simulation, in *Proc. Sixth Int. Heat Transfer Conf.*, Vol. 3, pp. 43–47. Hemisphere, Washington, D.C. (1978).
15. K. C. Cheng and S. L. Wong, Liquid solidification in a convectively cooled parallel-plate channel, *Can. J. Chem. Engng* **55**, 149–155 (1977).
16. K. C. Cheng and S. L. Wong, Asymmetric solidification of flowing liquid in a convectively cooled parallel-plate channel, *Appl. Scient. Res.* **33**, 309–335 (1977).
17. M. N. Özisik and J. C. Mulligan, Transient freezing of liquids in forced flow inside circular tubes, *J. Heat Transfer* **91**, 385–389 (1969).



18. P. G. Kroegen and S. Ostrach, The solution of a two-dimensional freezing problem including convection effects in the liquid region, *Int. J. Heat Mass Transfer* **17**, 1191–1207 (1974).
19. E. M. Sparrow, S. V. Patanka and S. Ramadhyani, Analysis of melting in the presence of natural convection in the melt region, *J. Heat Transfer* **99**, 520–526 (1977).
20. T. Saito, N. Seki and S. Ozaki, Studies on the freezing of flowing water over a flat plate, Preprints of the 5th Heat Transfer Symp. of Japan, pp. 157–160 (1968).
21. M. L. Miller, Two-dimensional solidification of viscous flow over a semi-infinite flat plate, Ph.D. Thesis, The City University of New York (1969).
22. R. R. Gilpin, H. Imura and K. C. Cheng, Experiments on the onset of longitudinal vortices in horizontal blasuis flow heated from below, *J. Heat Transfer* **100**, 71–77 (1978).
23. H. Schlichting, *Boundary Layer Theory*, 6th edn. McGraw-Hill, New York (1968).
24. L. M. Milne-Thomson, *Theoretical Hydrodynamics*, 5th edn, p. 172. MacMillan, New York (1968).
25. W. M. Kays, *Convective Heat and Mass Transfer*, p. 222. McGraw-Hill, New York (1966).
26. J. Kestin, The effect of free-stream turbulence on heat transfer rates, in *Advances in Heat Transfer*, Vol. 3, p. 1. Academic Press, New York (1966).
27. R. R. Gilpin, T. Hirata and K. C. Cheng, Longitudinal vortices in a horizontal boundary layer in water including the effects of the density maximum at 4°C, ASME Paper No. 78-HT-25 (1978).

#### PROFIL PERMANENT DE LA COUCHE DE GLACE SUR UNE PLAQUE A TEMPERATURE CONSTANTE, EN CONVECTION FORCEE: 1ère Partie—REGIME LAMINAIRE

**Résumé**—On étudie la forme de la couche de glace qui apparaît en régime permanent sur une plaque horizontale à température constante, dans un écoulement parallèle forcé. Dans cette première partie, on examine les phénomènes qui affectent la forme pour le régime laminaire. Les effets de courbure de la surface de la glace et de la conduction thermique longitudinale dans la couche de glace sont particulièrement intéressants. Un modèle bidimensionnel développé pour tenir compte d'eux, suggère l'utilisation d'un nombre de Reynolds modifié  $Re_x/\theta_c^2$  où  $\theta_c$  est un paramètre de température. On trouve que les mesures peuvent être unifiées par ce paramètre, pour un large domaine de température de plaque, de température d'écoulement libre et de vitesse d'écoulement. Dans le régime laminaire, des instabilités thermiques de la couche limite sont observées, lesquelles produisent des rainures longitudinales sur la surface de la glace.

#### DAS PROFIL DER STATIONÄREN EISSCHICHT AUF EINER PLATTE KONSTANTER TEMPERATUR BEI ERZWUNGENER STRÖMUNG—I. BEREICH DER LAMINAREN STRÖMUNG

**Zusammenfassung**—Die Form einer stationären Eisschicht, die sich auf einer horizontalen Platte konstanter Temperatur bei paralleler erzwungener Strömung bildet, wurde analysiert. Diese Arbeit, Teil I einer zweiteiligen Folge, wird die Phänomene, welche die Form der Eisschicht im Bereich der laminaren Strömung beeinflussen, untersuchen. Von besonderem Interesse sind die Einflüsse der Krümmung der Eisoberfläche auf die freie Strömung und die der Wärmeleitung der Eisschicht in Strömungsrichtung. Eine zweidimensionale Theorie, in der diese Einflüsse berücksichtigt werden, legt es nahe, eine modifizierte Reynolds-Zahl der Form  $Re_x/\theta_c$  zur Darstellung der Eisprofile zu verwenden, wobei  $\theta_c$  ein Temperaturverhältnisparameter ist. Es wurde gefunden, daß bei Verwendung dieses Parameters die Messungen in einem weiten Bereich von Plattentemperaturen sowie Temperaturen und Geschwindigkeiten der freien Strömung gut korreliert werden konnten. Auch im laminaren Bereich wurden thermische Instabilitäten der Grenzschicht beobachtet, die Längsrillen in der Eisoberfläche hervorriefen.

#### СТАЦИОНАРНЫЙ ПРОФИЛЬ СЛОЯ ЛЬДА НА ОБТЕКАЕМОЙ ПЛАСТИНЕ ПОСТОЯННОЙ ТЕМПЕРАТУРЫ. ЧАСТЬ I. ЛАМИНАРНЫЙ РЕЖИМ

**Аннотация** — Анализируется конфигурация стационарного слоя льда, образующегося на горизонтальной пластине, находящейся в параллельном потоке. В данной статье, представляющей собой первую часть работы, исследуются явления, оказывающие влияние на конфигурацию слоя льда при ламинарном режиме течения. Особое внимание обращено на влияние кривизны поверхности льда на свободный поток и теплопроводность слоя льда в направлении течения. Для учёта этих эффектов разработана двумерная модель, в которой для обобщения профилей слоя льда используется модифицированное число Рейнольдса вида  $Re_x/\theta_c^2$ , где  $\theta_c$  — параметр отношения температур. Найдено, что с помощью данного параметра результаты измерений можно обобщить для широкого диапазона температур пластины, температур и скоростей свободного потока. Следует отметить, что при ламинарном режиме течения наблюдались термические неустойчивости пограничного слоя, которые приводили к образованию продольных канавок на поверхности льда.